CONDENSED MATTER

Bound States in the Continuum in Magnetophotonic Metasurfaces

A. M. Chernyak[a], M. G. Barsukova[a], A. S. Shorokhov[a], A. I. Musorin[a, *], and A. A. Fedyanin[a]

[a] *Faculty of Physics, Moscow State University, Moscow, 119991 Russia*
***e-mail: musorin@nanolab.phys.msu.ru**

We analyze the enhancement mechanisms of magneto-optical effects in all-dielectric metasurfaces caused by the bound state in the continuum resonance. In a structure under study, a square lattice of bismuth substituted yttrium iron garnet nanodisks with an air hole displaced away from the disk axis, magneto-optical polarization and intensity effects reach 0.7° and 22%, respectively.

Resonant dielectric nanostructures are of great interest to modern nanophotonics [1]. Light scattering by low-loss high-index dielectric nanoparticles allows repeating optical effects previously discovered for plasmonic particles, but without energy dissipation for heating [2]. Metasurfaces composed of such dielectric nanoobjects support manipulating of phase and amplitude of the transmitted or reflected light [3]. Usually, in these structures, the resonance Q-factor is of an order of 10, which is not sufficient for practical applications such as filters [4] and sensors [5]. These values of Q-factor are due to high radiation losses, i.e., strong coupling between the resonant nanoparticle and external field. There are various ways to increase the quality factor up to 10^2-10^3 [6−10]. The key element of achieving high Q-factor is spectral overlapping of two resonances, e.g., Fano-resonances. A strong resonant response occurs upon "trapped" mode excitation known as "dark" mode [11] when they are overlapped with "bright" modes. Introducing asymmetry to the structure allows making modes radiative. The degree of asymmetry defines the coupling efficiency of these two resonances. Symmetry-forbidden state is called the bound state in the continuum (BIC) [12]. BIC state possesses the infinity Q-factor being a mathematician model only. In reality, small symmetry breaking leads to a transformation of this state to a quasi-BIC state with high Q-factor resonance in a spectrum [13]. An application of such resonances to optical systems opens up possibilities for new compact nanophotonic devices.

In order to act as an active device, a structure should be sensitive to external influence. One of such stimuli may be a dc-magnetic field, which has the advantage of non-invasiveness and fast response.

Dielectric nanoparticles supporting excitation of Mie resonances and placed in a magnetic field, enhance magneto-optical (MO) effects [14]. In mag-netophotonic and magnetoplasmonic metasurfaces near-field coupling between nanoparticles leads to additional enhancement of the magneto-optical effects upon spectral overlapping of resonances [15−17]. However, in previous works [15−17], the earned Q-factor was only in the order of 10. If the Q-factor is more significant than higher values of amplification can be expected. For the THz range, it was calculated that one hundred percent values of magnetic circular dichroism could be achieved when BIC are excited [18]. Taking aforesaid into account, the use of high-Q asymmetrical nanostructures (see Fig. 1) is promising for MO effects enhancement at optical frequencies. In this work, we performed a numerical simulation for a case of all-dielectric magnetic metasurfaces composed of nanodisks with broken symmetry. We demonstrated the enhancement of intensity and polarization magneto-optical effects upon excitation of the BIC resonance.

Numerical calculations are carried out with finite difference time domain technique in commercial software FDTD Solutions, Lumerical Inc. The simulation is implemented for a 3D system with periodic bound-
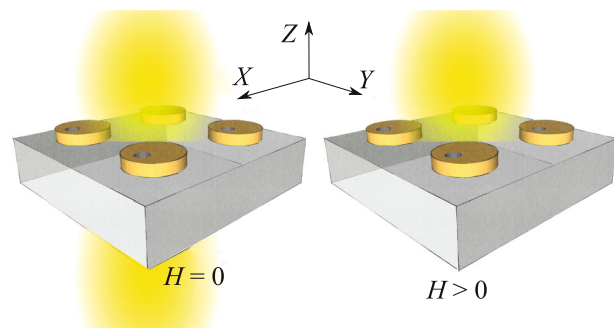

Fig. 1. (Color online) Sketch of the idea and the sample.

ary conditions on both *X*- and *Y*-axis, while along *Z*-axis perfectly matched layers are placed. Spectra are calculated for normal incidence of a plane electromagnetic wave along the *Z*-axis. The polarization direction is parallel to the *X*-axis. An external magnetic field is oriented along the *Y*-axis for Voigt geometry. A relative variance of transmittance is calculated according to the equation:

$$\delta = \frac{\Delta T}{T(0)} = \frac{T(H) - T(0)}{T(0)},$$

where $T(H)$ and $T(0)$ are transmittance spectra in case of the external dc-magnetic field and without it, respectively. The intensity effect manifests itself in a variation of the transmittance coefficient under applying the external magnetic field perpendicular to the polarization vector and the wave vector of the incoming light. The direction of external magnetic field is modified from *Y*- to *Z*-axis for the Faraday effect, which is polarization MO effect and results in polarization plane rotation θ by magnetized sample. The angle of the rotation is evaluated as the ratio of E_y/E_x in a far-field diffraction zone.

A two-dimensional square array of asymmetric nanodisks made of a magnetic dielectric, bismuth-substituted yttrium iron garnet (Bi:YIG, $n = 2.09$, $g = -0.001$), is simulated. The disks height $h = 227$ nm, and radius $R = 248$ nm. The disks are placed on a quartz substrate SiO_2 ($n = 1.45$). Every garnet nanodisk has a hole with the radius $r = 62$ nm. This hole is displaced from the disk center in the positive direction of the *Y*-axis. The asymmetry factor is defined as the ratio of this translocation y_0 to disk's radius R: $\alpha = y_0/R$. Period *d* in both directions is 679 nm. All these parameters lead to the existence of the quasi-BIC resonance in the vicinity of a wavelength of 1 um, while diffraction peculiarities are excluded from this region.

Simulations begin from a symmetric structure ($\alpha = 0$), when the hole is located at the garnet disk center. In this case, there is a localization of the field inside the disks (see Figs. 2e, 2f) corresponding to the resonance when the sample is being illuminated by a plane electromagnetic wave. Albeit the resonance dip in the transmittance spectrum is absent (see Fig. 2a and the blue curve in Fig. 3a). This case corresponds to a veritably BIC mode. As mentioned in the introduction, the perfect BIC state has infinite *Q*-factor, which explains the absence of the dip. The small symmetry disturbance by the hole displacement results in a transformation of BIC resonance to quasi-BIC mode with the following appearance of the dip in the transmittance spectrum (see Fig. 2a). Increasing asymmetry leads to a spectral shift of the resonance toward short wavelengths, its broadening, and *Q*-factor decreasing (see Fig. 2g). When the asymmetry parameter reaches a value $\alpha \sim 0.75$, the hole breaks the disk on the upper edge ($y = R = 248$ nm) and leads to
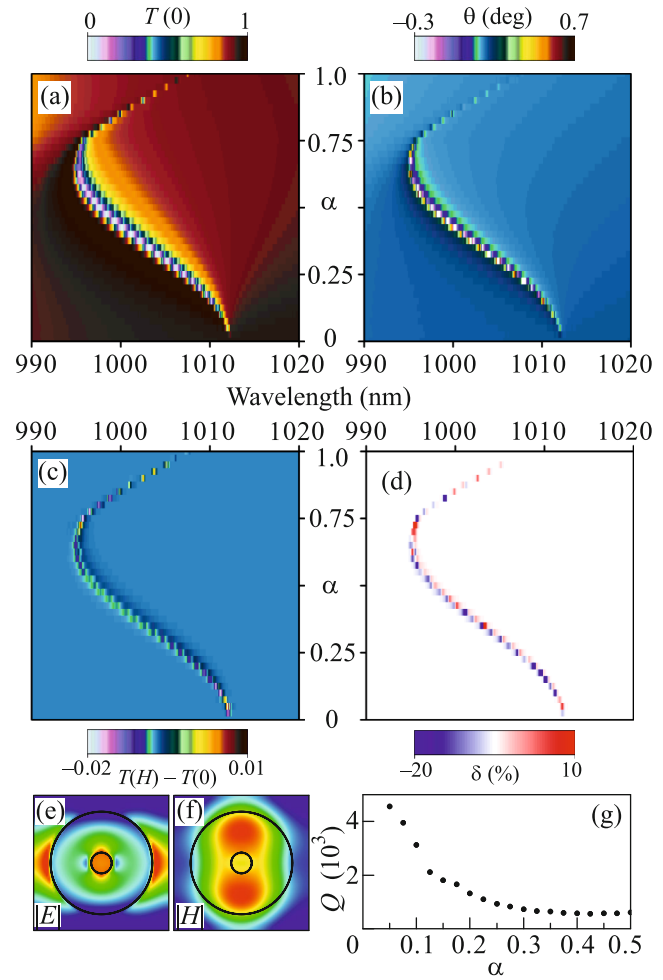

Fig. 2. (Color online) Spectra: (a) transmittance, (b) Faraday rotation, (c) differential transmittance ΔT, (d) Voigt effect, and (g) *Q*-factor as a function of the asymmetry factor α. The distributions of local electric (e) and magnetic (f) fields at the half height of the disk inside an elementary cell for α = 0.

the local electromagnetic field configuration disengagement. Following hole displacement leads to further modification of the transmittance spectrum. The transmittance dip moves toward larger wavelengths region, as the disk geometry becomes more symmetric, i.e., unperturbed. Figure 2b shows Faraday rotation spectra depending on the parameter α. Its variation results in the shift of enhanced magneto-optical signal following the dip in the transmittance spectrum. The angle θ is maximal for $\alpha = 0.225$ and reaches 0.7° (see Fig. 3b, red curve). The effect enhancement is 35 times larger compared with unstructured Bi:YIG film of the same thickness of 227 nm (θ = 0.02°). For every α, the maximal value of polarization plane rotation corresponds to the minimum of transmittance. It means that considered metasurface operates better on the slope of the resonance for polarization effects, where transmittance and Faraday rotation coexist.
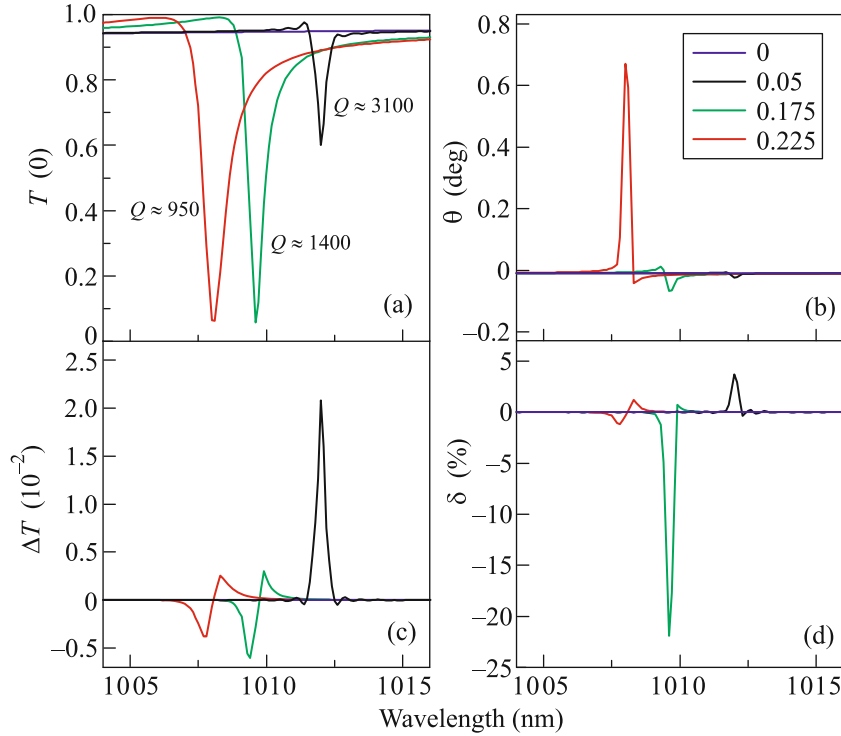
Fig. 3. (Color online) Spectra: (a) transmittance, (b) polarization effect, (c) differential transmittance $\Delta T = T(H) - T(0)$, (d) intensity effect for the models with the asymmetry factor $\alpha = 0$ (blue curve), 0.05 (black curve), 0.175 (green curve), 0.225 (red curve).

Results for the calculations of the intensity magneto-optical effect dependence on the parameter α are presented in Fig. 2d. The enhancement of the magneto-optical signal correlates with BIC mode resonance excitation. The maximal variation of transmittance reaches 22% for $\alpha = 0.175$ (see Fig. 3d, green curve). To avoid singularities during the calculations, caused by dividing on close to zero values of $T(0)$, graphs of transmittance difference with and without magnetic field ΔT are evaluated (see Fig. 2c). Moreover, differential transmittance ΔT represents the multiplication of the effect δ and optical transmittance without magnetic field $T(0)$, allowing one to find a position of simultaneously significant MO effect and transmittance. The most effective structure for ΔT maximization is the sample with the parameter $\alpha = 0.05$ (Fig. 3c, black curve), i.e., the metasurface with the highest Q-factor ($Q \approx 3100$).

It is known from the literature that polarization MO effects up to 0.06° were experimentally detected in lattices of magnetic particles supporting excitation of local plasmon and lattice resonances [19, 20]. Although ferromagnetic metals (like Fe, Ni) have high gyration coefficients, the value of MO response turns out small because of the considerable imaginary part of the dielectric permittivity of the metals. To avoid this problem, magnetic dielectric material exploited in this work is of great interest. The intensity magneto-optical effect with a magnitude of 0.015 with the transmittance of 0.4 was experimentally shown in 1D magnetoplasmonic crystal with a waveguiding garnet layer [21]. A similar system of 1D gold lattice embedded to a magnetic layer of EuS contributed experimental registration of Faraday rotation of 14°. However, such values were measured in magnetic fields of 5 T and under a temperature of 20 K, which limits the use of such samples in real life [22]. Proposed in this work all-dielectric magnetic metasurfaces composed of nanoparticles with broken symmetry demonstrate the values of the magneto-optical effects of the same or higher order as plasmonic and photonic-crystal samples. Bound state in the continuum leads to sharp, high-Q resonance allowing significantly enhance magneto-optical response of the system. The maximal value of polarization effect attained in this work is 0.7°, and for intensity effect it is 22%. The enhancement coefficient decreases with increasing of the asymmetry parameter because of the Q-factor decline. The optimal values of asymmetry should not exceed 0.25 for the practical applicability of nonreciprocal nanophotonics devices.

REFERENCES

1. A. I. Kuznetsov, A. E. Miroshnichenko, M. L. Brongersma, Y. S. Kivshar, and B. Luk'yanchuk, Science (Washington, DC, U. S.) **354** (6314), aag2472 (2016).

2. E. V. Melik-Gaykazyan, K. L. Koshelev, J. Choi, S. S. Kruk, H. Park, A. A. Fedyanin, and Y. S. Kivshar, JETP Lett. **109**, 131 (2019).

3. N. Yu and F. Capasso, Nat. Mater. **13**, 139 (2014).

4. Y. Lee, M. Park, S. Kim, J. H. Shin, C. Moon, J. Y. Hwang, J. Choi, H. Park, H. Kim, and J. E. Jang, ACS Photon. **4**, 1954 (2017).

5. A. A. Grunin, I. R. Mukha, A. V. Chetvertukhin, and A. A. Fedyanin, J. Magn. Magn. Mater. **415**, 72 (2016).

6. F. Hao, Y. Sonnefraud, P. V. Dorpe, S. A. Maier, N. J. Halas, and P. Nordlander, Nano Lett. **8**, 3983 (2008).

7. B. Luk'yanchuk, N. I. Zheludev, S. A. Maier, N. J. Halas, P. Nordlander, H. Giessen, and C. T. Chong, Nat. Mater. **9**, 707 (2010).

8. Y. Yang, I. I. Kravchenko, D. P. Briggs, and J. Valentine, Nat. Commun. **5**, 5753 (2014).

9. V. R. Tuz, V. V. Khardikov, A. S. Kupriianov, K. L. Domina, S. Xu, H. Wang, and H. Sun, Opt. Express **26**, 2905 (2018).

10. S. Campione, S. Liu, L. I. Basilio, L. K. Warne, W. L. Langston, T. S. Luk, J. R. Wendt, J. L. Reno, G. A. Keeler, I. Brener, and M. B. Sinclair, ACS Photon. **3**, 2362 (2016).

11. K. V. Baryshnikova, K. Frizyuk, G. Zograf, S. Makarov, M. A. Baranov, D. Zuev, V. A. Milichko, I. Mukhin, M. Petrov, and A. B. Evlyukhin, JETP Lett. **110**, 25 (2019).

12. K. Koshelev, S. Lepeshov, M. Liu, A. Bogdanov, and Y. Kivshar, Phys. Rev. Lett. **121**, 193903 (2018).

13. Y. Plotnik, O. Peleg, F. Dreisow, M. Heinrich, S. Nolte, A. Szameit, and M. Segev, Phys. Rev. Lett. **107**, 183901 (2011).

14. M. G. Barsukova, A. S. Shorokhov, A. I. Musorin, D. N. Neshev, Y. S. Kivshar, and A. A. Fedyanin, ACS Photon. **4**, 2390 (2017).

15. A. I. Musorin, M. G. Barsukova, A. S. Shorokhov, B. S. Luk'yanchuk, and A. A. Fedyanin, J. Magn. Magn. Mater. **459**, 165 (2018).

16. M. G. Barsukova, A. I. Musorin, A. S. Shorokhov, and A. A. Fedyanin, APL Photon. **4**, 016102 (2019).

17. A. I. Musorin, A. V. Chetvertukhin, T. V. Dolgova, H. Uchida, M. Inoue, B. S. Luk'yanchuk, and A. A. Fedyanin, Appl. Phys. Lett. **115**, 115102 (2019).

18. G. Y. Chen, W. X. Zhang, and X. D. Zhang, Opt. Express **27**, 16449 (2019).

19. M. Kataja, T. K. Hakala, A. Julku, M. J. Huttunen, S. van Dijken, and P. Törmä, Nat. Commun. **6**, 7072 (2015).

20. N. Maccaferri, X. Inchausti, A. García-Martín, J. Cuevas, D. Tripathy, A. O. Adeyeye, and P. Vavassori, ACS Photon. **2**, 1769 (2015).

21. L. E. Kreilkamp, V. I. Belotelov, J. Y. Chin, S. Neutzner, D. Dregely, T. Wehlus, I. A. Akimov, M. Bayer, B. Stritzker, and H. Giessen, Phys. Rev. X **3**, 041019 (2013).

22. D. Floess, M. Hentschel, T. Weiss, H. Habermeier, J. Jiao, S. G. Tikhodeev, and H. Giessen, Phys. Rev. X **7**, 021048 (2017).